AN EXPERIMENTAL INVESTIGATION OF FORCED CONVECTION FLAT PLATE SOLAR AIR HEATER WITH STORAGE MATERIAL

by

Walid AISSA [a*], ***Mostafa EL-SALLAK*** [b], ***and Ahmed ELHAKEM*** [a]

[a] Mechanical Power Department, High Institute of Energy, South Valley University, Aswan, Egypt
Curently Faculty of Engineering, Rabigh, King Abdulaziz University, KSA
[b] Mechanical Power Engineering Department, Faculty of Engineering, Cairo University, Cairo, Egypt

Original scientific paper
DOI: 10.2298/TSCI110607006A

Solar air heater is a heating device that uses the heated air in the drying of agriculture products and many engineering applications. The purpose of the present work is to study a forced convection flat plate solar air heater with granite stone storage material bed under the climatic conditions of Egypt-Aswan. Experiments are performed at different air mass flow rates; varying from 0.016 kg/s to 0.08 kg/s, for five hot summer days of July 2008. Hourly values of global solar radiation and some meteorological data (temperature, pressure, relative humidities, etc.) for measuring days are obtained from the Egyptian Meteorological Authority, Aswan station. Inlet and outlet temperatures of air from a solar air heater have been recorded. In this work, attempt has been made to present the temperature distribution in non-dimensional form that makes it useable for any region and not restricted to local conditions. The variation of solar radiation, air heater efficiency, Nusselt number, and temperature distribution along the air heater are discussed. Comparisons between the calculated values of outlet air temperatures, average air temperatures and storage material temperatures and the corresponding measured values showed good agreement. Comparison between current work and those in previous investigations showed fair agreement.

Key words: *solar air heater, forced convection, performance, efficiency*

Introduction

The inability to preserve food surpluses, which is the main reason of food problem in most developing countries, leads to 30-40% losses of fruits and vegetables [1, 2]. Drying basically reduces the moisture content, hence prevents the development of a suitable environment for the growth of moulds, bacteria and insects that cause spoilage of agriculture products [3, 4].

Natural Sun drying method is commonly used for the drying of agricultural products in developing countries using solar radiation and the air's enthalpy available in the ambient environment. Hence, the drying cost is minor [2, 3]. However, natural sun drying may be accompanied by negative impacts like contaminations, birds, insects, rain, storms, microorganisms, and other problems [4-6]. These drawbacks can be solved using a solar dryer which consists of air heater, dryer chamber and, sometimes, a chimney [3].

* Corresponding author; e-mail: walidaniss@gmail.com

In developing countries, various small scale solar dryers were designed and evaluated in space heating, drying of agricultural products and paint spraying operations. High percentage of these dryers use Sun or wind as energy sources. The airflow can be generated by either natural or forced-convection [7-8].

The use of appropriate solar dryers leads to energy savings, lower manufacturing labor requirements, reduction of the drying time, enhancement of the product quality (color, texture, and taste) [7], without emitting SO_2, NO_x, and CO_2 [9]. Absorption of heat by the product supplies the energy necessary for dewatering of the product [10].

The air heater is a major component of a solar food drying system. Hence, understanding of the performance of of air heaters would lead to the design of high performance solar dryers [5].

Solar energy systems are usually installed at an angle from the horizontal surface to increase the solar energy angle of incidence on the surface of the air heaters. The angle of inclination is a design constraint locked to the geographical latitude. The optimum tilt angle should be 0.9 times of the latitude of the location. The inclination of the heater can be as much as ±20° to favor winter or summer collection [11]. Different optimal tilt angles correspond to different months of a year [12, 13]. The thumb rule for optimum inclination of the solar air heater (SAH) states that the optimum inclination of the solar air collector to maximize the capture of solar radiation is equal to latitude angle ±15°[14]. In the northern hemisphere, the optimum orientation for SAH is south facing.

Hence, the air heater in the current investigation is oriented to face south and tilted 24º with respect to the horizontal during the five testing days in Aswan, Egypt (23º 58' N and 32º 47' E).

Comparison of experimental studies (natural convection *vs.* forced convection) have shown that forced convection dryers are preferred because they cause an increase of local heat flux and temperature rise, offer better control for more uniform drying and also because of their high air heater efficiency [15].

In the present study, forced convection flat plate SAH is constructed and investigated experimentally and analytically in five sunny days (2nd July, 3rd July, 4th July, 5th July and 6th July 2008). The effects of varying air mass flow rate on its performance is discussed. Air mass flow rates corresponding to the five testing days are 0.08, 0.064, 0.048, 0.032, and 0.016 kg/s respectively. In this work, attempt has been made to present the temperature distribution in non-dimensional form that makes it useable for any region and not restricted to local conditions. To the best of our knowledge, no work in the literature is represented in this form. The experimental results are compared with the previous works in order to verify and monitor how this may predict the experimental results obtained.

Description of SAH

A cross-sectional view of the SAH is shown in fig. 1. An electrical centrifugal blower (0.75 kW, 2 m^3/s, 2800 rpm) is used to deliver air with a constant flow rate to the air heater. Ambient air which is sucked by the electrical centrifugal blower, flows through an intermediate tunnel to enter the SAH. The tunnel has internal guide vanes to ensure uniform distribution of the air over the width of the air heater.

SAH has ($2.10 \times 0.84 \times 0.369$ m^3) outer dimensions. The top of the SAH is covered with a single transparent glass layer. High transmissivity to solar radiation glass cover; (0.005 m thickness) is used because glass is the most common glazing material used for drying. The gap spacing

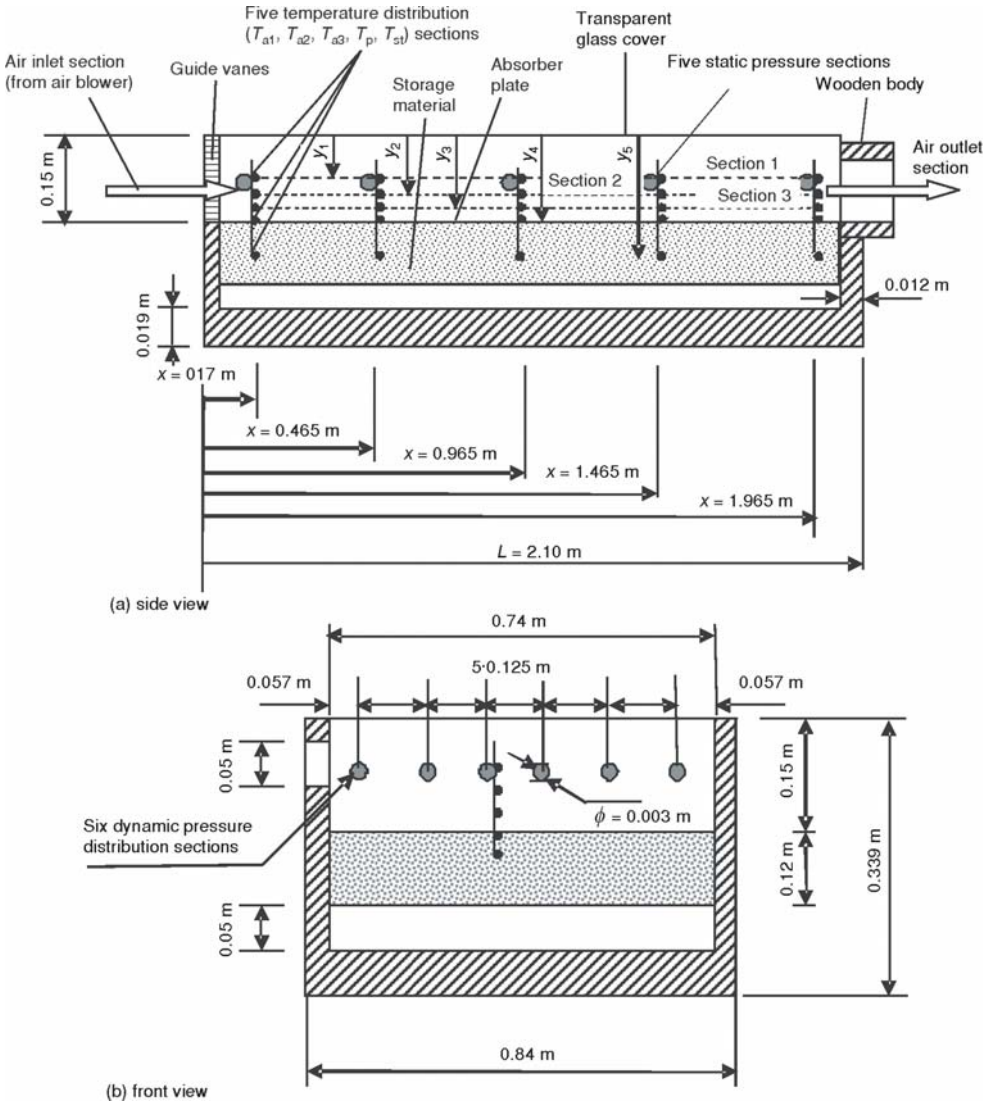

Figure 1. Air heater sections and locations of the measuring parameters (not in scale)

between the absorber plate and the glass cover is about 0.15 m. The air heater frame is constructed from wooden plate of 0.012 m thickness except at the bottom which has 0.019 m thickness. The upper surface of absorber plate; which is made of aluminum plate having 0.0015 m thickness, is painted with matt black layer to increase the absorptivity of the solar radiation and thereby reduces the temperature gradient between the inside and outside surfaces. The air is heated while passing between the transparent glass cover and absorber plate. A layer of storage material (granite stones) is bedded underneath the absorber plate with 0.12 m thickness. As it was indicated in the literature [5], the storage layer stores the heat during sun-period and rejects the heat during off-sunshine period. Hence, it accelerates the drying process, especially during low solar radiation intensity and off-sunshine periods [16].

The system is insulated from all sides and bottom by a 0.05 m thickness fine wood frame to reduce the heat losses to ambient air. The whole air heater is oriented to face south and tilted 24º with respect to the horizontal to maximize the solar radiation incident on the air heater.

Experimentation

The experiments are conducted to investigate many important performance parameters of SAH such as temperature distribution, Nusselt number, and air heater efficiency.

The SAH inlet is exposed to ambient air so that the inlet air temperature and pressure were equal to the ambient values. The air running through the air heater is pre-heated to approx. 10-25 °C above ambient temperature before leaving to the dryer chamber. The measurement variables are:

– air temperatures – T_{a1}, T_{a2}, and T_{a3}, plate temperature – T_p, and storage material temperature – T_{st} located at vertical distances (y_1, y_2, y_3, y_4, and y_5) measured from transparent glass cover of (0.07 m, 0.10 m, 0.125 m, 0.15 m, and 0.21 m), respectively,
– dynamic pressure locations – p_{01}, p_{02}, p_{03}, p_{04}, p_{05}, and p_{06}, and
– static pressure locations – p_1, p_2, p_3, p_4, and p_5.

The temperatures and pressures of the different elements of the system are recorded every one hour.

Instrumentation

Pressure measuring instruments

– Digital micro manometer

Digital micro manometers are used to measure low pressure. The pressure is measured by a pressure load cell with a membrane spring, which is displaced according to the pressure difference between the two points in the pressure load cell. A calibrated digital micro manometer; Testo 512 type (measuring range = 0 to 200 Pa, accuracy = 0.5% of full scale, resolution = 0.1 Pa) is used in pressure measurements in the current investigation.

– Pitot tube

The difference between the dynamic and static heads at the inlet section of the air heater; measured by Pitot tube, leads to the evaluation of the velocity at this point. The density of air, cross-sectional area of the air heater and mean velocity at inlet section of air heater are used to calculate the air mass flow rate.

The pressure difference between each individual point in the six dynamic pressure points across the cross-section of the air gap for each static pressure section and the corresponding static pressure point present at the mid cross-section of the air gap is used to evaluate the velocity at the concerned point. Velocity at different points is evaluated by switching the On/Off valves connecting the dynamic pressure measuring points to the high pressure port in the digital micro manometer and the On/Off valves connecting the static pressure measuring points to the low pressure port in the digital micro manometer. Five 0.02 m × 0.05 m ports are present on one side of the air heater; fig. 1(b), at same longitudinal distances from the air heater inlet section as those of the five static pressure sections. The five dynamic pressure tubes and the corresponding static pressure tube corresponding to each pressure section are extracted from the air heater through the corresponding port to reduce the interference with air flow.

Temperature measurement

A calibrated hygro-thermometer (YF-180) having K(CA)NiAl/NiCr thermocouple TP-02 type of –50 °C to 1300 °C measuring range, resolution = 1°C and accuracy = ±(0.5%, +1°C), is used to measure the temperature. The sensor probe of this unit is equipped with a portable external plug to measure the room temperature (0 °C-60 °C) and humidity (10%-95% RH). Dust protection cover is used to extend the life span and function of the sensor. Five terminals corresponding to air temperatures – T_{a1}, T_{a2}, and T_{a3}, plate temperature – T_p, and storage material temperature – T_{st} at each temperature distribution section are extracted from a hole in the transparent glass cover nearly at the mid cross-section of the air heater at that temperature distribution section to reduce the interference with the flow.

Pressure ports on the side of the air heater and temperature holes in the glass cover are sealed to minimize the leakage and reserve the heat capacity.

Thermal analysis

The following analytical expressions are obtained for the outlet and average temperatures of the flowing air with storage materials [16]:

$$T_{\text{fos}} = T_{\text{fs}}(x,t)\big|_{x=L} = \left(\frac{\overline{f_2(t)}}{b_2}\right)\left\{1-\exp\left[-\left(L+\frac{t}{a_1}\right)\left(\frac{b_2}{2}\right)\right]\right\} + T_{\text{fis}}\exp\left[-\left(L+\frac{t}{a_1}\right)\left(\frac{b_2}{2}\right)\right] \quad (1)$$

and

$$T_{\text{favs}} = \left(\frac{1}{L}\right)\int_0^L T_{\text{fs}}(x,t)\,\mathrm{d}x = \frac{\overline{f_2(t)}}{b_2} + \frac{\overline{2f_2(t)}}{Lb_2^2}\exp\left[-\left(\frac{b_2 t}{2a_1}\right)\right]\left[\exp\left(-\frac{b_2 L}{2}\right)-1\right] + \frac{2T_{\text{fis}}}{b_2 L}\exp\left[-\left(\frac{b_2 t}{2a_1}\right)\right]\left[1-\exp\left(-\frac{b_2 L}{2}\right)\right] \quad (2)$$

where T_{fos} and T_{favs} are the outlet and average temperatures of flowing air with storage material, t is the time, x – the longitudinal distance along the flat plate in the flow direction, L – the air heater length, and T_{fis} – the air initial temperature with storage. The coefficients a_s, b_s, and functions $f_s(t)$ are summarized in [16].

The following analytical expression is obtained for the storage material [16]:

$$T_{\text{st}}(t) = \left(\frac{\overline{f_3(t)}}{a_2}\right)[1-\exp(a_2 t)] + T_{\text{sti}}\exp(-a_2 t) \quad (3)$$

where T_{sti} is the initial storage temperature, $T_{\text{sti}} = T_{\text{st}}$ (t = 0), and $\overline{f_i(t)}$, is the average of $f_i(t)$ over a selected time interval.

Average local Nusselt number for fully developed flow in smooth air heater is calculated as [17]:

$$\text{Nu} = \frac{\left(\frac{f}{8}\right)(\text{Re}-1000)\,\text{Pr}}{1+12.7\sqrt{\frac{f}{8}}\left(\sqrt[3]{\text{Pr}^2}-1\right)} \quad (4)$$

where average local air Prandtl and Reynolds numbers; Pr and Re are dimensionless numbers defined using the following relations:

$$\mathrm{Pr} = \frac{\nu}{\alpha} \tag{5}$$

$$\mathrm{Re} = \frac{4R_{\mathrm{H}}V}{\nu} \tag{6}$$

where, α, ν, and V are average local air thermal diffusivity, kinematic viscosity and velocity, respectively. R_{H} – the hydraulic radius, area to perimeter ratio, computed based on the air heater cross-section; (0.74 m × 0.15 m in the current investigation).

The friction factor; f is given by [17]:

$$f = \frac{1}{(1.82\log \mathrm{Re} - 1.64)^2} \tag{7}$$

The thermal efficiency of an air heater is a measure of how effectively the solar energy collected is transferred to and flowing through the air heater. Mathematically, the average efficiency of SAH; η_{c} is defined as the ratio of the useful thermal energy to the total incident solar radiation averaged over the same time interval. It is expressed as [1]:

$$\eta_{\mathrm{c}} = \frac{\dot{m}c_p \int_{t_1}^{t_2} (T_{\mathrm{o}} - T_{\mathrm{in}})\,\mathrm{d}t}{A_{\mathrm{c}} \int_{t_1}^{t_2} I_{\mathrm{T}}\mathrm{d}t} \tag{8}$$

where c_p is the average specific heat capacity of air at constant pressure, T_{o} – the air heater outlet temperature, T_{in} – the air heater inlet temperature, I_{T} – the solar radiation per unit area on the air heater's tilted plane, and t_1 and t_2 are initial and final measuring times.

One of the main problems in the design of solar dryers is that the solar radiation received on a tilted plane I_{T} is not known for most sites. Instead, the solar radiation received on a horizontal plane I is traditionally recorded in meteorological stations. Vlachos *et al.* [18] employed a general procedure in order to deduce I_{T} from available local measurements of solar radiation on a horizontal plane. For the matter of simplicity, I_{T} is substituted by I in the current work.

Air mass flow rate, $\dot{m}$, is:

$$\dot{m} = \rho V A_{\mathrm{c}} \tag{9}$$

where ρ is the average density of the air, A_{c} – the cross-section area of the air heater, and V – the air average velocity.

Results and discussion

Local measured data of global solar radiation incident on a horizontal surface and some meteorological data (temperature, pressure, relative humidities, *etc*.) on July 2nd- 6th, 2008 (testing days) obtained by direct contact with Egyptian Meteorological Authority, Aswan station, are utilized in this work. The hourly variation of solar intensity – I and ambient air temperature – T_{amb} for the testing days are shown in figs. 2 and 3, respectively.

From the results in figs. 2 and 3, it is seen that for the second day, the solar radiation increases with the time of day until reaching its maximum value of 1259 W/m^2 at 1 p. m. Similar behaviors have been observed during the first and third days. Ambient temperatures exhibit the same behavior as the solar radiation. However, they achieve their maximum values of 46.0, 47.0,

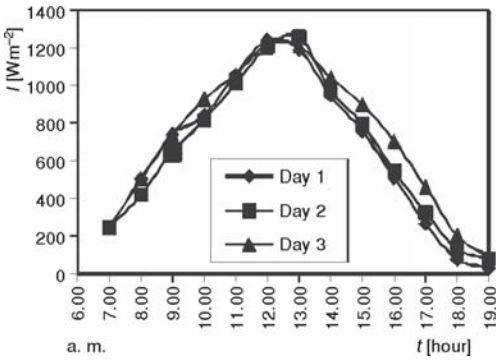

Figure 2. Hourly variation of solar radiation in three measuring days, Day 1, Day 2, and Day 3

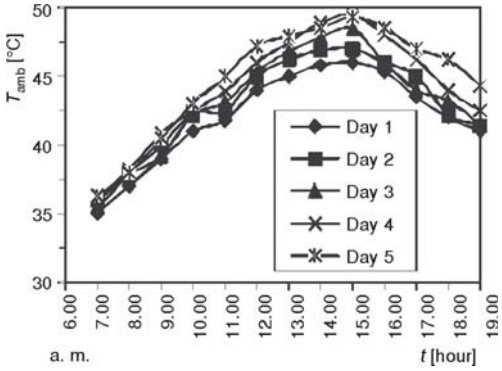

Figure 3. Ambient air temperature in all run days

48.5, 49.5, and 49.3 °C at 3 p. m. The observed ambient temperature ranged between 35.0 °C and 49.5 °C during the period of experimentation. Daily average values of solar radiation and ambient temperature are obtained as 677.3 W/m^2 and 42.3 °C, respectively.

Figures 4 , 5, and 6 illustrate the variation of dimensionless temperatures of air at section 1, at absorber plate and storage material (θ_{a1}, θ_p, and θ_{st}), respectively, along the air heater. It may be remarked that θ_{a1}, θ_p, and θ_{st} in general increase along the air heater. Experimental results indicated that sections 2 and 3 nearly have the same trend as section 1. Measured data illustrated that the maximum air temperatures are obtained in the interval from 12:00 a. m. to 4:00 p. m. where solar radiation is maximum, with peak value are nearly at 1:00 p. m. In all results, it was observed that the absorbed plate exhibited the highest temperature.

It may be concluded from figs. 4-6 that dimensionless temperatures in general increase with the increase of solar radiation. This can be explained as follows: For a certain value of Re, an increase in the incident radiation flux increases the temperature level of the absorber plate

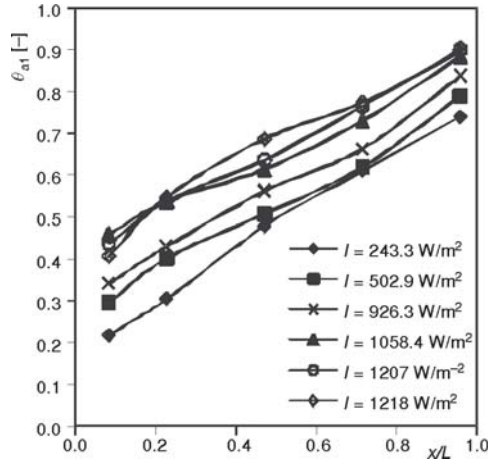

Figure 4. Variation of dimensionless measured air temperature at section 1 along the air heater; $\dot{m}$ = 0.048 kg/s

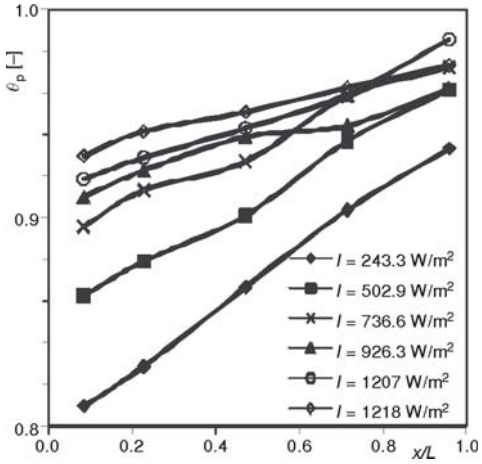

Figure 5. Variation of dimensionless measured absorber plate temperature along the air heater; $\dot{m}$ = 0.048 kg/s

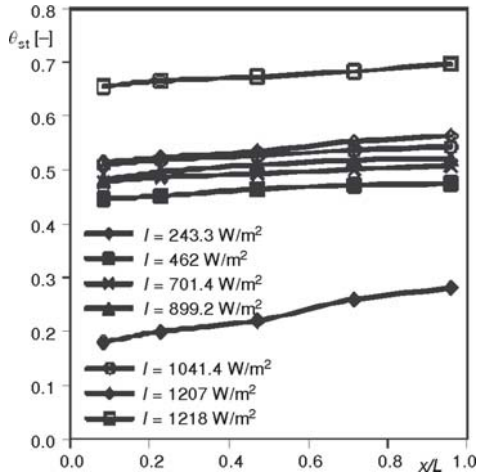

Figure 6. Variation of dimensionless measured storage material temperature along the air heater; $\dot{m}$ = 0.048 kg/s

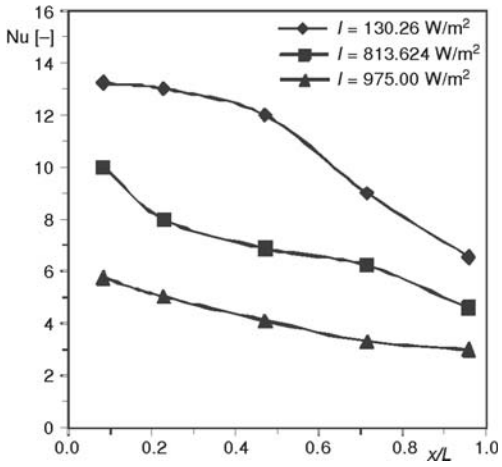

Figure 7. Longitudinal variation of Nusselt number in air heater for different values of solar radiation; $\dot{m}$ = 0.064 kg/s

that has an effect on both the velocity and the air thermal boundary layers development. The higher temperature of the absorber plate increases the near wall air and storage material temperatures. This matches the findings presented in [19].

Figure 7 is a sample figure illustrating spatial variation of Nusselt number for different values of solar radiation. As it was indicated in [19] that Nusselt number decreases along the air heater. It may be remarked from fig. 7 that the maximum value of Nusselt number occurs at the entry section of the air heater which is mostly affected by heat transfer from the wall and inside circumference of the air heater. Further, it may be concluded that the heat transfer decreases by the increase of solar radiation. Increase of the solar radiation leads to higher temperature of the absorber plate and to the increase of the near wall air temperature, and consequently, to the increase of the air viscosity. This increase in air viscosity affects the wall shear stress and decreases the local Re as well which causes an increase in thermal boundary layer thickness, and results in decreasing the convective heat transfer coefficient. This matches the findings presented in [19].

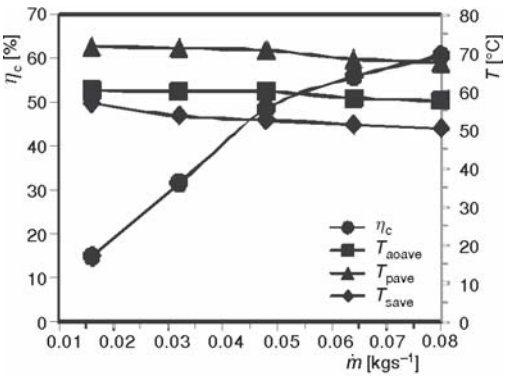

Figure 8. Variation of air heater average outlet air temperature, absorber plate and storage material temperatures at outlet section and efficiency with mass flow rate

Figure 8 illustrates the variation of average outlet air temperature, absorber plate and storage material temperatures at outlet section and air heater efficiency with air mass flow rate. The SAH outlet temperature; which nearly equals the dryer chamber inlet temperature, is an important parameter for drying purpose because it essentially affects solar batch drying time. Increase of heated air temperature considerably reduces the drying time. It may be observed from fig. 8 that the average outlet air temperature decreases with increasing air mass flow rate until mass flow rate equals 0.048 kg/s.

With further increase of mass flow rate, average outlet air temperature decreases with higher rate. This is due to the fact that when the air flow rate increases, the amount of air to be heated with the same quantity of solar energy increases.

Solar radiation through the transparent sheet causes the temperature of the air; flowing in the air heater to rise internally due to green house effect [15]. It may be observed from figs. 3 and 8 that the rise of the outlet air temperature from the air heater above the ambient air temperature is in the range of 10-25 °C during the testing runs. The range of the rise above the ambient air in [3, 18, 20, and 21] are 5-20 °C, 10-20 °C, 11-15 °C, and 16-21 °C, respectively.

The difference in the range of temperature rise above the ambient air in the different works may be attributed to the mass flow rate, incident radiation and operating conditions.

Further, it may be observed that increasing the air mass flow rate causes a decrease in plate and storage material temperatures. This may be due to cooling effect of the air to plate and storage material rather than heating when exceeding mass flow rate beyond a certain limit.

As it was indicated in [22], for a specific air heater; hence a specific transmittance of the cover; and air heater mean absorption coefficient, the thermal efficiency of air heater depends basically on air mass flow rate. It is shown from fig. 8 that the air heater efficiency is strongly dependent on mass flow rate, it increases with increasing mass flow rate $\dot{m}$ until a typical value of 0.048 kg/s. Beyond 0.048 kg/s, the efficiency increases with a lower rate. This is not surprising and reflects the energy balance in the heater as the residence time of flowing air gets lower at high air flow rates.

The above mentioned observations indicate that for drying purpose, the recommended range of air mass flow rate which gives an appropriate outlet air temperature suitable for drying of most agriculture drying applications; 60-70 °C as it was indicated in [6], is 0.03-0.048 kg/s. The efficiency corresponding to the recommended air mass flow rate range is considered reasonable.

The uncertainty in a result is calculated on the basis of the uncertainties in the measurements of all the related independent variables [23]. An uncertainty analysis is performed, and the uncertainty in Nusselt number and air heater efficiency are found to be ±4.95% and ±4.567%, respectively.

Comparison of experimental results with theoretical prediction

Figure 9 shows an example of comparisons between measured outlet air temperatures, average air temperatures and storage material temperatures for air heater and those calculated using the mathematical model presented by Aboul-Enein *et al.* [16], outlined in thermal analysis section in the present work. It is obvious that there is good agreement between the calculated and measured values. In all cases, the percentage differences between the calculated and measured temperatures do not exceed 4.05%, 6.6%, 5.4%, 9.76%, and 17.72% for Day1, Day2, Day3, Day4, and Day5, respectively.

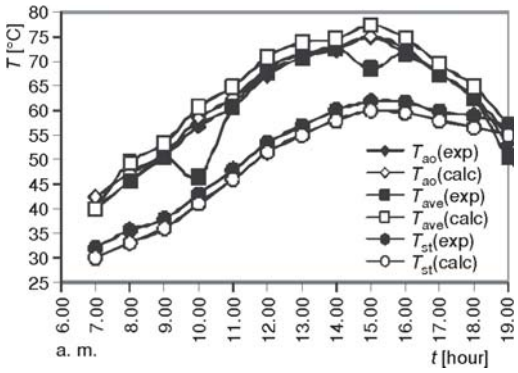

Figure 9. Comparisons between the calculated and measured values of outlet air, average air and storage material temperatures in air heater for Day1

Solar radiation and outlet air temperature presented in figs. 2 and 9 nearly exhibit the same behavior of solar radiation and outlet air temperature reported by Shanmugam and Natarajan [24]. Comparing figs. 2 and 9 may indicate that that the temperatures of the various elements increase with time as the solar radiation increases. It is important to note that the maximum temperature is achieved after 3:00 p. m., fig. 9, while the maximum radiation is reached at 1:00 p. m., fig. 2. This time lag may be due to the inertia of the system.

For the matter of fact, the following investigation contains some simplifying hypotheses. First, the measurements take time to perform and are by no means simultaneous as the authors have supposed. Also, the solar radiation received on a tilted plane I_T is substituted by the solar radiation received on a horizontal plane I. However, it was remarked that the variations in the measured pressure and temperature in the testing period are within the accuracy of the measuring instruments. Hence, it may be claimed that the measurements were conducted for quasi steady flow. Further, Vlachos, *et al.* [18] illustrated that the discrepancy between I_T and I increases with increasing the air heater tilt angle and that the discrepancy for 60° tilt angle is greater than that for 45° tilt angle which in turn is greater than that for 30° tilt angle. Hence, assuming that $I_T \approx I$ is somehow accepted approximation in the current investigation in which the tilt angle is 24°. Therefore, this work is too simple, but complete, to model and comprehend the thermal behavior of the solar air heater submitted to real climatic conditions.

Conclusions

On the basis of the experimental and theoretical results obtained for five run days for forced convection SAH manufactured and tested in High Institute of Energy, South Valley University, Aswan, Egypt, the following conclusions can be drawn.

- Air, plate and storage material temperatures in general increase along the air heater.
- Air mass flow rate and solar radiation are predominant factors which affect the performance of SAH. Increasing the air mass flow rate causes a consequent decrease of air, plate, and storage material temperatures.
- For drying purpose, the recommended range of air mass flow rate which gives an appropriate outlet air temperature and thermal efficiency is 0.03-0.048 kg/s.
- Present experimental results showed good and fair agreements with corresponding theoretical results and those in pervious investigations, respectively.
- The rise of the outlet air temperature from the air heater above the ambient air temperature is in the range of 10-25 °C during the testing runs.

Acknowledgments

The authors are grateful to the Egyptian Meteorological Authority, Aswan station, for providing the global solar radiation and some meteorological data. The authors wish to express their cordial thanks to the referees for their valuable suggestions and comments which led to the improvement of the paper.

Nomenclature

A – cross-sectional area, [m^2]
c_p – average specific heat, [$Jkg^{-1}K^{-1}$]
f – friction factor, [–]
I – solar radiation per unit area received on an horizontal plane, [Wm^{-2}]
I_T – solar radiation per unit area on the air heater's tilted plane, [Wm^{-2}]

L – length, [m]
$\dot{m}$ – air mass flow rate, [kgs^{-1}]
Nu – local average Nusselt number, [–]
Pr – local average Prandtl number, [–]
Re – local average Reynolds number, [–]
T – temperature, [K]
t – time, [s]
V – average velocity, [ms^{-1}]
x – distance along air heater, [m]

Greek symbols

α – thermal diffusivity, [m^{2}s^{-1}]
ϕ – diameter, [m]
ν – local average kinematic viscosity, [m^{2}s^{-1}]
ρ – average density, [kgm^{-3}]
η_c – air heater efficiency, [–]
θ – dimensionless temperature; $\theta = (T - T_{in})/(T_o - T_{in})$, [–]

Subscripts

a – air
amb – ambient
ave – average
c – collector (air heater)
favs – fluid (air) average with storage material
fis – fluid (air) initial with storage material
fos – fluid (air) outlet with storage material
fs – fluid (air) with storage material
in – inlet
o – outlet
p – plate
save – storage material average
st – storage material
sti – initial, storage material

Acronym

SAH – solar air heater

References

[1] Karim, M. A., Hawlader, M. N. A. Development of Solar Air Collectors for Drying Applications, *Energy Conversion and Management, 45* (2004), 3, pp. 329-344
[2] Ekechukwu, O. V., Norton, B. Experimental Studies of Integral-Type Natural-Circulation Solar-Energy Tropical Crop Dryers, *Energy Convers. Mgmt, 38* (1997), 14, pp. 1483-1500
[3] Janjai, S., Tung, P., Performance of a Solar Dryer Using Hot Air from Roof-Integrated Solar Collectors for Drying Herbs and Spices, *Renewable Energy, 30* (2005), 14, pp. 2085-2095
[4] Ayensu, A., Dehydration of Food Crops Using a Solar Dryer with Convective Heat Flow, *Solar Energy, 59* (1997), 4-6, pp. 121-126
[5] El-Sebaii, A. A., *et al*., Experimental Investigation of an Indirect Type Natural Convection Solar Dryer, *Energy Conversion and Management, 43* (2002), 16, pp. 2251-2266
[6] Thanvi, C. K. P., Pande, P. C., Development of a Low-Cost Solar Agricultural Dryer for Arid Regions of India, *Energy in Agriculture, 6* (1987), 1, pp. 35-40
[7] Esper, A., Muhlbauer, W., Solar Drying-An Effective Means of Food Preservation, *Renewable Energy, I5* (1998), 1-4, pp. 95-100
[8] El-Sawi, A. M., *et al*., Application of Folded Sheet Metal in Flat Bed Solar Air Collectors, *Applied Thermal Engineering, 30* (2010), 8-9, pp. 864-871
[9] Stefanović, V. P., Bojić, M. Lj., Development and Investigation of Solar Collectors for Conversion of Solar Radiation into Heat and/or Electricity, *Thermal Science, 10* (2006), Suppl., 4, pp. 177-187
[10] Ekechukwu, O. V., Norton, B., Review of Solar-Energy Drying Systems II: An Overview of solar Drying Technology, *Energy Conversion & Management, 40* (1999), 6, pp. 615-655
[11] Henderson, D., *et al*., Experimental and CFD Investigation of an ICSSWH at Various Inclinations, *Renewable and Sustainable Energy Reviews,11* (2007), 6, pp. 1087-1116
[12] Dragićević, S. M., Vučković, N. M., Evaluation of Distributional Solar Radiation Parameters of Čačak Using Long-Term Measured Global Solar Radiation Data, *Thermal Science, 11* (2007), 4, pp. 125-134
[13] Luminosu, I., De Sabata, C., But, A., Solar Equipment for Preheating Bitumen, *Thermal Science, 11* (2007), 1, pp. 127-136
[14] Jain, D., Jain, R. K., Performance Evaluation of an inclined Multi-Pass Solar Air Heater with In-Built Thermal Storage on Deep-Bed Drying Application, *Journal of Food Engineering, 65* (2004), 4, pp. 497-509
[15] Abdullah, M. O., Mikie, F. A., Lam, C. Y., Drying Performance and Thermal Transient Study with Solar Radiation Supplemented by Forced-Ventilation, *International Journal of Thermal Sciences, 45* (2006), 10, pp. 1027-1034

[16] Aboul-Enein, S., *et al*., Parametric Study of a Solar Air Heater with and without Thermal Storage for Solar Drying Applications, *Renewable Energy, 21* (2000), 3-4, pp. 505-522
[17] Lienhard IV, J. H., Lienhard V, J. H., A Heat Transfer Text Book, 3rd ed., Phlogiston Press, Cambridge, Mass., USA, 2004
[18] Vlachos, N. A., *et al*., Design and Testing of a New Solar Tray Dryer, *Drying Technology, 20* (2002), 5, pp. 1239-1267
[19] Ali, A. H. H., *et al*., Experimental Study of Laminar Flow Forced-Convection Heat Transfer in Air Flowing through Offset Plates Heated by Radiation Heat Flux, *Int. Comm. Heat Mass Transfer, 25* (1998), 3, pp. 297-308
[20] Arinze, E. A. , Schoenau, G. J., Sokhansanj, S., Design and experimental evaluation of a solar dryer for commercial high-quality HAY production, *Renewable Energy, 16* (1999), 1-4, pp. 639-642
[21] Arinze, E. A., *et al*., Design and Experimental Evaluation of a New Commercial Type Mobile Solar Grain Dryer Provided with High Efficiency Fined-Plate Collector, *WREC* (1996), 1-4, pp. 670-675
[22] Kadam, D. M., Samuel, D. V. K., Convective Flat-Plate Solar Heat Collector for Cauliflower Drying, *Biosystems Engineering, 93* (2006), 2, pp. 189-198
[23] Figliola, R. S., Beasley, D. E., Theory and Design for Mechanical Measurements, 2nd ed., John Wiley and Sons, New York, USA, 1995
[24] Shanmugam, V., Natarajan, E., Experimental Investigation of Forced Convection and Desiccant Integrated Solar Dryer, *Renewable Energy, 31* (2006), 8, pp. 1239-1251

Paper submitted: June 6, 2011
Paper revised: January 11, 2012
Paper accepted: January 16, 2012